Climate System Responses to a Common Emission Budget of Carbon Dioxide

DI TIAN,[+] WENJIE DONG,[#,@] XIAODONG YAN,[+] JIEMING CHOU,[+] SHILI YANG,[+] TING WEI,[&] HAN ZHANG,[*,**] YAN GUO,[+] XIAOHANG WEN,[++] AND ZHIYONG YANG[+]

[*] *State Key Laboratory of Satellite Ocean Environment Dynamics, Second Institute of Oceanography, Hangzhou, China*
[+] *State Key Laboratory of Earth Surface Processes and Resource Ecology, Beijing Normal University, Beijing, China*
[#] *School of Atmospheric Sciences, Sun Yat-Sen University, Guangzhou, China*
[@] *Zhuhai Joint Innovative Center for Climate-Environment-Ecosystem, Future Earth Research Institute, Beijing Normal University, Zhuhai, China*
[&] *Chinese Academy of Meteorological Sciences, Beijing, China*
[**] *State Key Laboratory of Marine Environmental Science, College of Ocean and Earth Sciences, Xiamen University, Xiamen, China*
[++] *Plateau Atmosphere and Environment Key Laboratory of Sichuan Province, College of Atmospheric Sciences, Chengdu University of Information Technology, Chengdu, China*

(Manuscript received 20 March 2015, in final form 5 January 2016)

ABSTRACT

Global warming as quantified by surface air temperature has been shown to be approximately linearly related to cumulative emissions of CO_2. Here, a coupled state-of-the-art Earth system model with an interactive carbon cycle (BNU-ESM) was used to investigate whether this proportionality extends to the complex Earth system model and to examine the climate system responses to different emission pathways with a common emission budget of man-made CO_2. These new simulations show that, relative to the lower emissions earlier and higher emissions later (LH) scenario, the amount of carbon sequestration by the land and the ocean will be larger and Earth will experience earlier warming of climate under the higher emissions earlier and lower emissions later (HL) scenario. The processes within the atmosphere, land, and cryosphere, which are highly sensitive to climate, show a relatively linear relationship to cumulative CO_2 emissions and will attain similar states under both scenarios, mainly because of the negative feedback between the radiative forcing and ocean heat uptake. However, the processes with larger internal inertias depend on both the CO_2 emissions scenarios and the emission budget, such as ocean warming and sea level rise.

1. Introduction

Anthropogenically driven increase in CO_2 related to fossil fuel use and land-use changes has been identified as the primary forcing factor contributing to global warming that has occurred since the industrial revolution (IPCC 2007, 2013). Global warming caused by CO_2 will be almost irreversible on human time scales, even if emissions of CO_2 cease (Matthews and Caldeira 2008; Plattner et al. 2008; Solomon et al. 2009, 2010; Gillett et al. 2011; Zickfeld et al. 2013; Frölicher et al. 2014). This indicates that past, present, and future emissions of CO_2 will cause a substantial multicentury climate change (IPCC 2013).

Ongoing changes in extreme weather and climate events, such as heat waves, high sea levels, and heavy precipitation, suggest that global warming represents a large potential risk for ecological systems, as well as for human well-being and development. Therefore, many studies have examined climate stabilization and the long-term climate target (Hansen et al. 2008; Allen et al. 2009; Meinshausen et al. 2009; Zickfeld et al. 2009; Ramanathan and Xu 2010; Matthews et al. 2012). Today, a global warming threshold of 2°C above the preindustrial level is widely adopted as a guiding principle for mitigation efforts aimed at reducing the risk of the harmful effects of climate change (Meinshausen et al. 2009). A near-linear relationship between global

Corresponding author address: Wenjie Dong, School of Atmospheric Sciences, Sun Yat-Sen University, No. 19, XinJieKouWai St., Guangzhou 510000, China.
E-mail: dongwj@bnu.edu.cn

DOI: 10.1175/JCLI-D-15-0213.1

Publisher's Note: This article was revised on 8 June 2016 to correct errors in the affiliations of the first two authors.

mean temperature change and cumulative CO_2 emissions has been identified in many studies (Allen et al. 2009; Matthews et al. 2009; Gillett et al. 2013; Cherubini et al. 2014; Friedlingstein et al. 2014). This relationship has been named the transient climate response to cumulative CO_2 emissions (TCRE), defined as the ratio of global mean surface temperature change to cumulative emissions of CO_2 at the time of doubling in a 1% yr^{-1} CO_2 increase experiment (Gillett et al. 2013). Allen et al. (2009) pointed out that the relationship between cumulative emissions and peak warming is remarkably insensitive to the emission pathway, based on simulations of simple climate–carbon cycle models. Matthews et al. (2009) demonstrated that the TCRE is approximately independent of both the atmospheric CO_2 concentration and its rate of change. Previously, Caldeira and Kasting (1993) had pointed out that the global warming potential of CO_2 is nearly independent of the CO_2 emission scenario. Hence, any given level of peak warming is associated with a given budget of CO_2 emissions; that is, higher emissions earlier imply lower emissions and stronger reductions later.

The approximate proportional relationship between cumulative emissions and warming has been widely used in studies of climate change mitigation policy and formulation of targets for emissions reduction (Rogelj et al. 2013; Friedlingstein et al. 2014; Knutti and Rogelj 2015). The Intergovernmental Panel on Climate Change (IPCC) Fifth Assessment Report (AR5; IPCC 2013) calculated that limiting the warming caused by anthropogenic CO_2 emissions alone to less than 2°C since the period 1861–80, with a probability of >66%, will require that the upper cumulative CO_2 emissions from all anthropogenic sources remain below about 1000 GtC. An amount of 515 (445–585) GtC had already been emitted by 2011, meaning that the remaining quota on carbon emissions is less than 500 GtC. How to reasonably allocate the remaining and limited quota on carbon emissions over time and between countries is the key issue of the future research (Raupach et al. 2014; Knutti and Rogelj 2015).

Most previous research on the relationship between cumulative emissions of CO_2 and climate stabilization has focused on the relationship between emission targets and warming quantified by surface air temperature. However, the responses of other processes in the atmosphere, land, ocean, and cryosphere have received less attention (Herrington and Zickfeld 2014). To date, most studies about TCRE have focused on either idealized and "realistic" future emissions pathways where CO_2 emissions increase monotonically (Eby et al. 2013; Gillett et al. 2013; IPCC 2013; Raupach 2013; Frölicher and Paynter 2015; Goodwin et al. 2015) or those where CO_2 is emitted at a constant rate (Nohara et al. 2013; Krasting et al. 2014; MacDougall and Friedlingstein 2015), and they have used simple (Allen et al. 2009; Goodwin et al. 2015) or intermediate-complexity (Matthews et al. 2009; Eby et al. 2013) climate models coupled, or even decoupled, with carbon-cycle feedback. To our knowledge the validity of the TRCE in a declining emissions scenario remains to be fully assessed by using a comprehensive Earth system model. Therefore, we address these shortcomings in this study and investigate whether the approximately linear relationship between global warming and cumulative carbon emissions can be extended to a declining emissions scenario and to other processes within the climate system from the perspective of the historical anthropogenic CO_2 emissions over the twentieth century. To fully represent the net responses of the earth system to anthropogenic CO_2 emissions, a fully coupled state-of-the-art Earth system model (BNU-ESM) that accounts for the carbon-cycle feedback is used (Ji et al. 2014). Two different pathways that lead to a common cumulative CO_2 emission target are emphasized in this article: lower emissions earlier and higher emissions later (LH) and higher emissions earlier and lower emissions later (HL).

2. Model and experiments

a. Model description

The Beijing Normal University–Earth System Model (BNU-ESM, version 1) is a fully coupled Earth system model. It contributed to phase 5 of the Coupled Model Intercomparison Project (CMIP5) and provided future climate projections for IPCC AR5. This model can reasonably simulate the present-day climate (Wei et al. 2012; Dong et al. 2013). BNU-ESM contains four separate models that can simultaneously simulate Earth's atmosphere (CAM3.5), ocean (MOM, version 4.1), land surface [BNU Common Land Model (CoLM3)], and sea ice (CICE, version 4.1), as well as one central coupler component [(NCAR CCSM3 coupler, version 6 (CPL6)]. It has a global dynamic vegetation submodel and terrestrial carbon and nitrogen cycles based on the Lund–Potsdam–Jena model and the Lund–Potsdam–Jena dynamic nitrogen scheme in the land component as well as an idealized ecosystem–biogeochemical module in the ocean component. Hence, modeled atmospheric CO_2 concentrations are fully coupled to land and ocean CO_2 fluxes. The horizontal resolution of the atmosphere is T42 spectral truncation (approximately 2.81° × 2.81° transform grid), with 26 levels in the vertical and using hybrid sigma–pressure coordinates. The horizontal resolution of the ocean is 1° × 1°, with 50 isopycnic layers in the vertical (Ji et al. 2014).

b. Experiment design and method introduction

We designed two numerical experiments based on the BNU-ESM. These two experiments were run over the

period 1850–2005. 1) For the LH scenario experiment, the historical industrial CO_2 emission flux from fossil fuel combustion and cement production (Andres et al. 2011) is used. The non-CO_2 forcing agents (i.e., non-CO_2 greenhouse gases, aerosols, solar irradiance, and volcanoes) and the carbon emissions from land-use changes are kept constant at the 1850s levels (defined as preindustrial). The carbon emission rate from land-use changes is about 0.5 Pg C yr^{-1}, according to the data provided by CMIP5 (http://cmip-pcmdi.llnl.gov/cmip5/forcing.html). 2) The HL scenario experiment is similar to LH but uses a reverse time series of the historical industrial CO_2 emission flux. The cumulative total carbon emissions for the simulated period were the same in these two experiments. The yearly CO_2 emissions in the LH scenario were lower first and higher later, indicating an earlier reduction in CO_2 emissions, whereas in the HL scenario, the CO_2 emissions were higher first and lower later, indicating a later reduction in CO_2 emissions (Fig. 1). In addition, a corresponding preindustrial control run of 258 years and the globally averaged atmospheric CO_2 concentration from 1850 to 2005 provided by CMIP5 (http://cmip-pcmdi.llnl.gov/cmip5/forcing.html) were used to evaluate the BNU-ESM.

3. Results

a. Carbon cycle and terrestrial ecosystems

CO_2 removed from the atmosphere is absorbed by the land biosphere and ocean on multiple time scales—usually decades for land biosphere and surface ocean and centuries for the deep ocean (Archer et al. 2009; Joos et al. 2013). Figure 2 shows that the cumulative carbon sequestration by land and ocean increases with the cumulative manmade CO_2 emissions and is pathway dependent, which is consistent with earlier studies (Gregory et al. 2009; Le Quéré et al. 2009; Arora et al. 2013; Wei et al. 2014), suggesting that the carbon cycle is sensitive to the emission scenario. Relative to the LH scenario, the global cumulative carbon uptake by the land biosphere, as a result of net ecosystem productivity, is larger under the HL scenario, resulting from the more effective CO_2 fertilization mechanism under this scenario (Peng et al. 2013). By 2005, the net ecosystem productivity of the terrestrial ecosystem is 115 Pg C under LH and 160 Pg C under HL. The cumulative net carbon uptake by the ocean is smaller under the HL scenario before cumulative CO_2 emissions reach about 290 Pg C. This feature is highly associated with the longer time scale for ocean carbon uptake.

The relationships between the airborne fraction of anthropogenic CO_2 and the cumulative emissions are

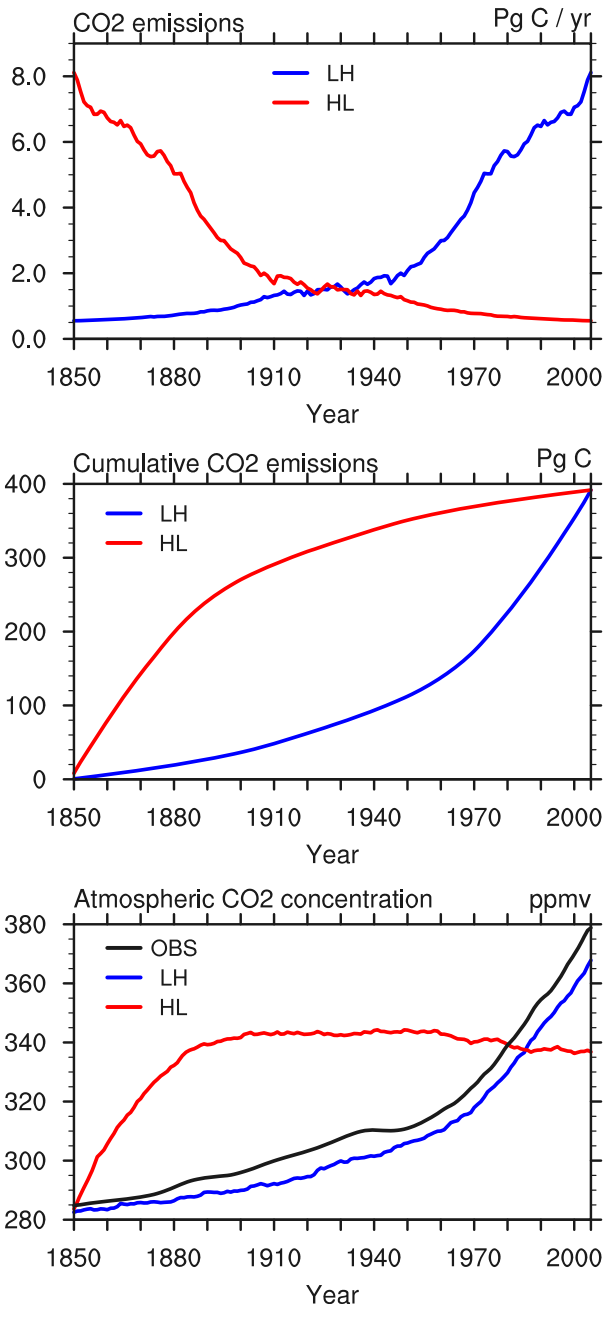

FIG. 1. (top) Annual total CO_2 emissions (Pg C yr^{-1}), (middle) cumulative CO_2 emissions (Pg C), and (bottom) global annual mean atmospheric CO_2 concentration (ppmv) as simulated in the LH (blue) and HL (red) experiments. The variables are shown as a global total, except for CO_2 concentration. OBS indicates the observed atmospheric CO_2 concentration.

different under the LH and HL scenarios (Fig. 2). The CO_2 airborne fraction tends to be constant under the LH scenario and decreases with the cumulative emissions under the HL scenario. By the end of the simulations, the CO_2 airborne fraction is relatively smaller under the

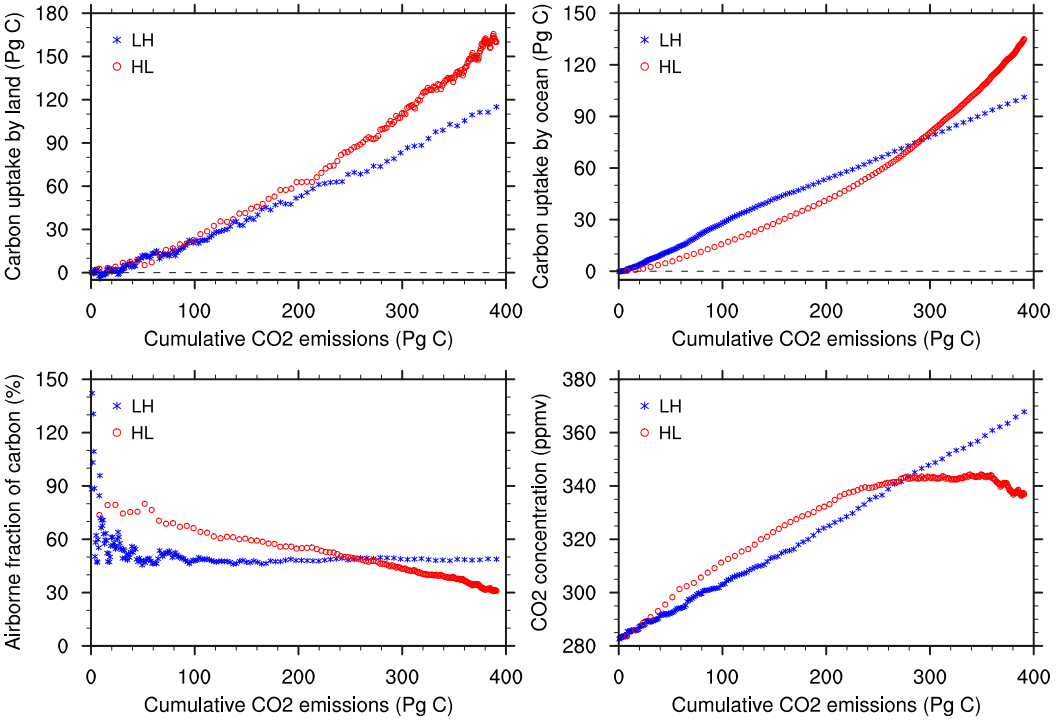

FIG. 2. (top left) Land cumulative net carbon uptake (Pg C), (top right) ocean cumulative net carbon uptake (Pg C), (bottom left) airborne fraction of carbon (%), and (bottom right) atmospheric CO_2 concentration (ppmv) vs the cumulative CO_2 emissions (Pg C) under the LH (blue) and HL (red) scenarios.

HL scenario (about 50% under LH and 30% under HL), resulting from the more effective CO_2 fertilization mechanism in combination with the more effective ocean carbon sequestration under this scenario. Therefore, by 2005, because of the larger amount of the cumulative carbon sequestration by land and ocean under the HL scenario, the atmospheric CO_2 concentration under this scenario was about 30 ppm by volume (ppmv) lower than it is under the LH scenario. Note that the historical land-use changes, one of the important anthropogenic carbon sources, shows a trend of 0.79 Pg C $(100\,\text{yr})^{-1}$ ($p < 0.05$). As land-use change emission rate is kept at the 1850s level in the simulations, the simulated atmospheric CO_2 under LH is expected to be lower than the observation (Fig. 1).

Because of the different responses of the terrestrial carbon cycle under the LH and HL scenarios (Fig. 2), the responses of the leaf area index and the relevant leaf-surface evapotranspiration are slightly different under these two scenarios (Fig. 3). Relative to the HL scenario, the leaf area index under the LH scenario is closer to being linearly increasing along with the cumulative industrial CO_2 emissions. When the CO_2 emission budget is less than about 310 Pg C, the leaf area index and leaf-surface evapotranspiration are slightly larger under the HL scenario.

b. *Climate*

The time evolutions of the climate responses are different under these two different CO_2 emission pathways (not shown). Earth would experience a warmer climate during nearly the whole simulated period under the HL scenario, which resulted in a faster hydrological cycle. Relative to the LH scenario, the global annual-mean surface air temperature and total precipitation averaged over the period 1850–2005 are 0.37°C and 0.63% greater under HL, respectively. These differences are larger than the model internal variabilities, 0.14°C for surface air temperature and 0.44% for precipitation. Differences in the responses of sea ice extent and snow cover between these two scenarios, averaged over 1850–2005, are also larger than the model internal variabilities (Table 1). However, many aspects of the climate system, such as the atmosphere, land, and cryosphere, can attain similar states by the end of the simulation period under these two different scenarios. For the last decade of the simulations, the differences between the HL and LH scenario are only about 0.07°C for global mean surface air temperature, 0.37% for precipitation, $-0.40 \times 10^6\,\text{km}^2$ for sea ice extent, and $-0.55 \times 10^6\,\text{km}^2$ for snow cover, which are within the model internal variabilities (Table 1).

Figure 4 shows the responses of the impact-relevant Earth system parameters, such as surface air temperature,

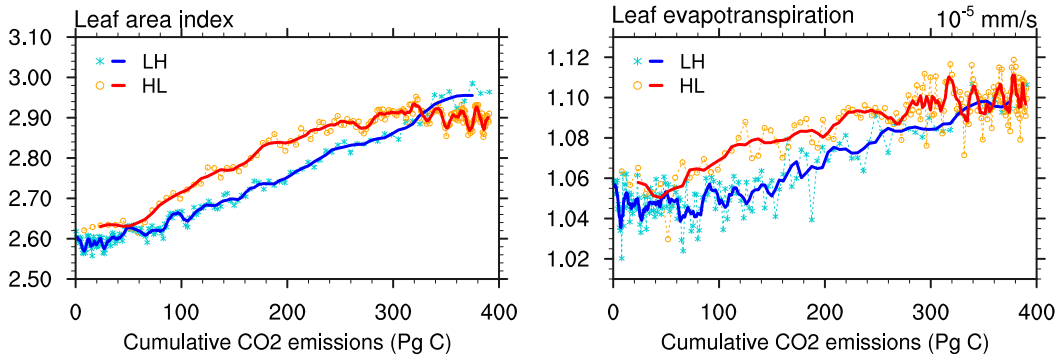

FIG. 3. Responses of (left) leaf area index and (right) leaf evapotranspiration (10^{-5} mm s^{-1}) vs the cumulative CO_2 emissions (Pg C) under the LH (blue) and HL (red) scenarios. The markers are the annual mean and the solid lines are the 5-yr running-averaged fields.

precipitation, sea ice extent, snow cover, upper-ocean heat content, and sea level height, plotted as the function of cumulative CO_2 emissions. The changes of surface air temperature, precipitation, sea ice extent, and snow cover, which are highly sensitive to the radiative forcing, all have an approximately linear relationship with the cumulative CO_2 emissions under both the LH and HL scenarios. Moreover, the surface radiative and nonradiative fluxes also show a nearly linear relationship to the cumulative CO_2 emissions, especially for the surface net radiative flux and surface upward latent heat, which are directly associated with the responses of surface air temperature and precipitation, respectively (Fig. 5). In addition, the difference in radiative forcing between these two scenarios caused by the different levels of atmospheric CO_2 is largely offset by the adjustment in land and ocean heat uptake; that is, the net heat uptake by land and ocean is smaller when the atmospheric CO_2 concentration is lower. Figure 5 indicates that the adjusted surface net radiative flux (the product of the radiative and nonradiative energy balance components at the surface) is slightly lower under the HL scenario for an emission budget of more than 320 Pg C, in accordance with the lower atmospheric CO_2 concentrations under the HL scenario. Specifically, relative to the LH scenario, ocean net heat uptake averaged over the last decade of the simulation period was 1.2 W m^{-2} smaller under HL, larger than the model internal variability (0.5 W m^{-2}), and mainly resulting from adjustments in sensible heat (-0.7 W m^{-2}) and latent heat (-0.3 W m^{-2}) fluxes into the ocean, which would compensate, in part, for the smaller radiative forcing caused by the lower atmospheric CO_2 concentration over that period. This is consistent with previous studies indicating that the smaller radiative forcing is largely compensated by the lower ocean heat uptake, which is considered to be negative feedback (Dufresne and Bony 2008; Gregory and Forster 2008; Solomon et al. 2010). Hence, this indicates that the responses of these processes within the climate system are related almost linearly to the cumulative CO_2 emissions but have little relationship with the emission scenario (Allen et al. 2009; Matthews et al. 2009; Gillett et al. 2013).

Because of the large ocean thermal inertia, the ocean's responses, such as upper-ocean heat content (0–700 m) and sea level height, are nonlinearly related to the cumulative CO_2 emissions but are closely related with emission scenarios, suggesting significantly different final states for the ocean (Fig. 4). It is well known that the ocean takes longer time to adjust to the external forcing than do the atmosphere and land. The time scale for ocean heat uptake is on the order of decades to centuries, similar to the time scale for ocean carbon sequestration. This effect is why the cumulative ocean heat uptake is smaller under the HL scenario relative to the LH scenario, when the amount of the cumulative CO_2 emissions is less than about 280 Pg C. Under the LH scenario, the upper-ocean heat content almost linearly increases with the increased cumulative CO_2 emissions.

TABLE 1. Differences of climatic variables between the HL and LH scenarios and the model internal variability evaluated by a 258-yr preindustrial simulation.

Variables	1850–2005 (HL minus LH)	1996–2005 (HL minus LH)	Model internal variability
Surface air temperature (°C)	0.37	0.07	0.14
Precipitation (%)	0.63	0.37	0.44
Sea ice extent (10^6 km^2)	1.16	−0.40	0.76
Snow cover (10^6 km^2)	1.15	−0.55	0.61

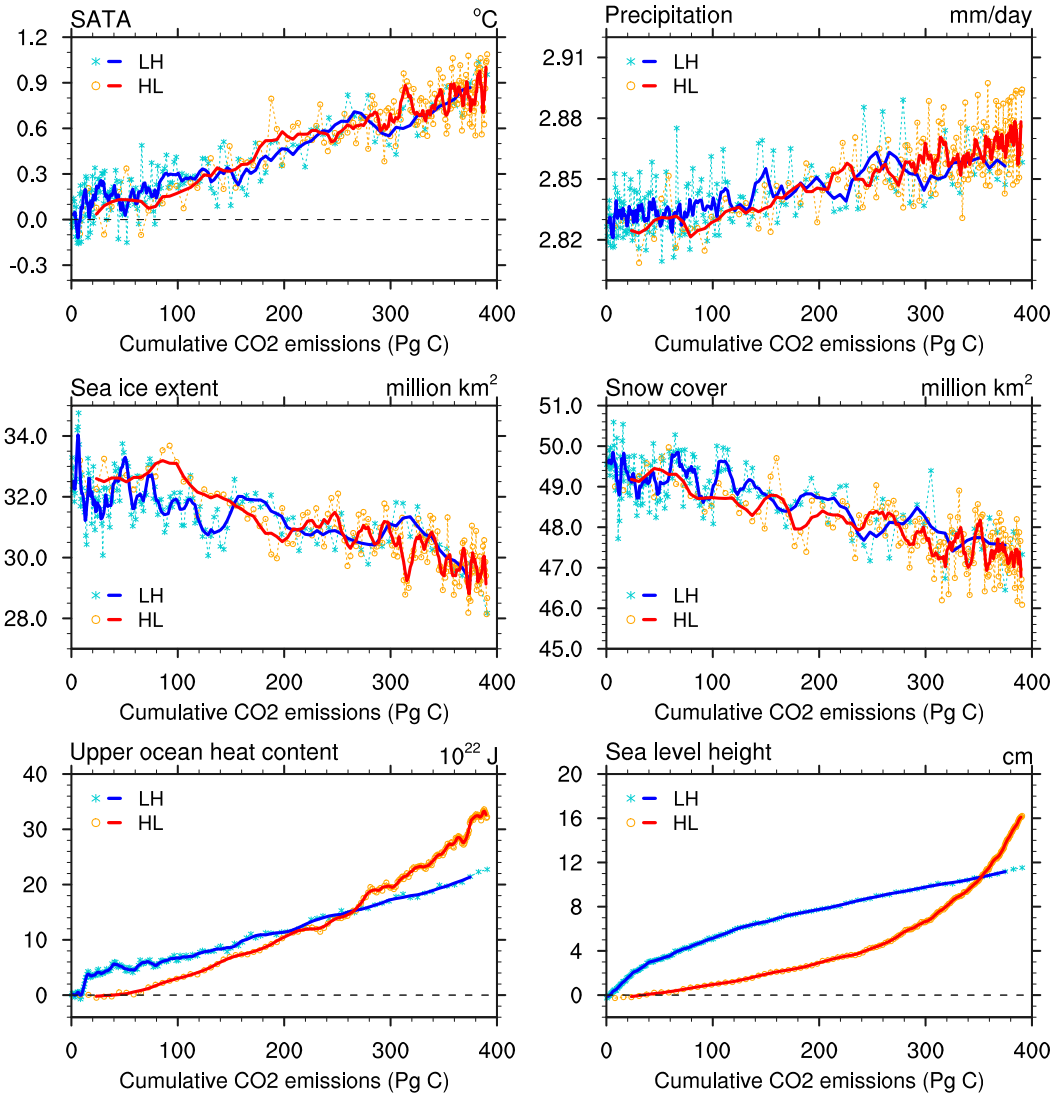

FIG. 4. Responses of climatic variables vs the cumulative CO_2 emissions (Pg C) under the LH (blue) and HL (red) scenarios: (top left) global mean surface air temperature anomalies (°C), (top right) global mean precipitation (mm day^{-1}), (middle left) global sea ice extent (10^6 km), (middle right) global snow cover (10^6 km), (bottom left) global upper-ocean heat contents (0–700 m; 10^{22} J), and (bottom right) global mean sea level rise (cm). The markers are the annual mean and the solid lines are the 5-yr running-averaged fields.

However, it exponentially increases with the cumulative CO_2 emissions under the HL scenario. For the whole simulated period, more heat is transported from the ocean surface to the subsurface and deep ocean under the HL scenario, relative to the LH scenario. Averaged over the period 1850–2005, the ocean heat uptake was 0.18 W m^{-2} greater under HL than under LH, resulting from changes in latent heat (−0.48 W m^{-2}), sensible heat (0.27 W m^{-2}), longwave radiation (0.46 W m^{-2}), and shortwave radiation (−0.08 W m^{-2}) fluxes into the ocean. By the end of the simulations, the differences between the HL and LH scenarios are about 9.5×10^{22} J for the upper-ocean heat content (0–700 m) and 45×10^{22} J for the whole-ocean heat content. The much larger cumulative ocean heat uptake over the simulated period under HL induces more ocean warming under this scenario, which may affect the ocean circulation. Figure 6 indicates that the extra heat absorbed by the ocean under the HL scenario is mainly stored in the tropical ocean around 500 m in depth and in the deep ocean at the high northern latitudes. The tropical ocean warming is mainly due to the shallow meridional circulation cell, which can transport more energy into the subsurface, while the deep warming north of 60°N is mainly due to

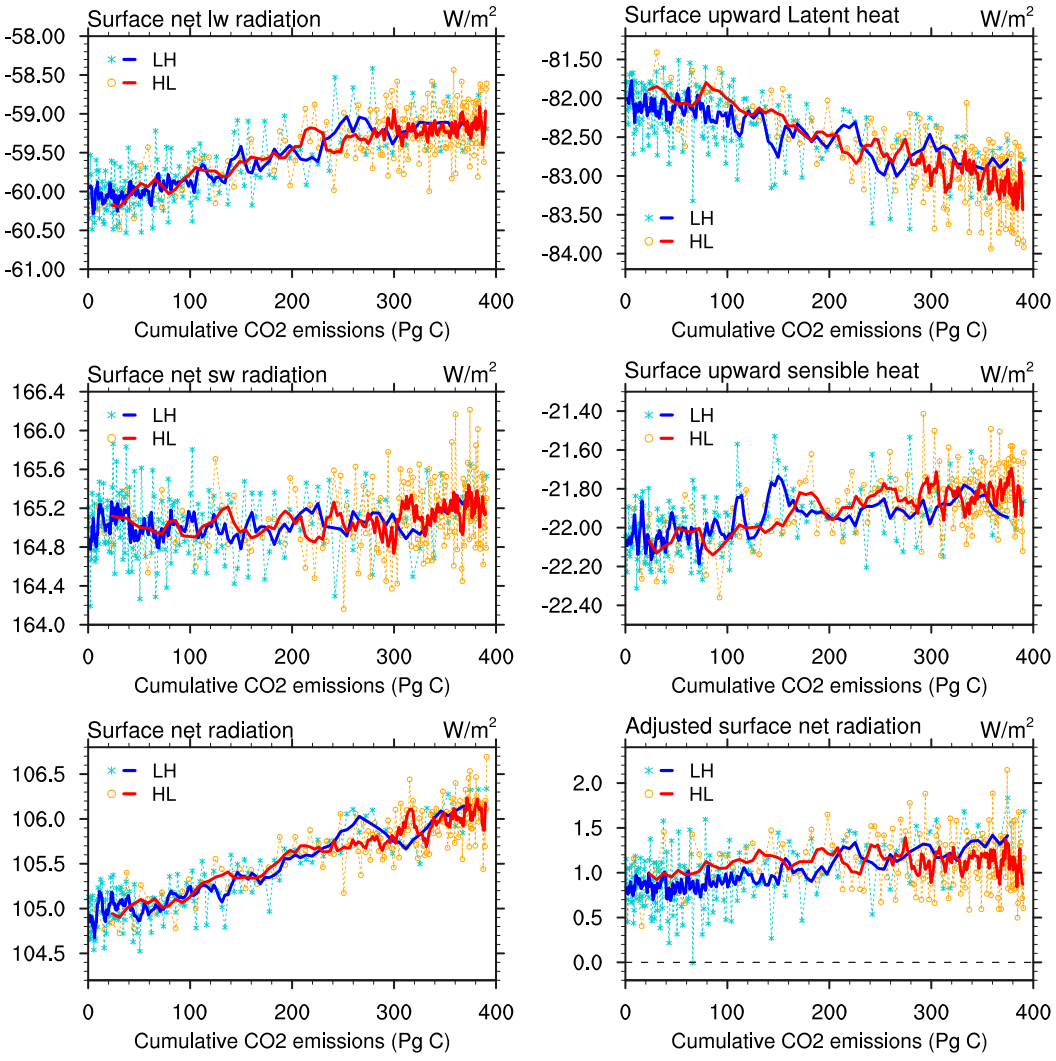

FIG. 5. Responses of radiative and nonradiative energy balance components at surface (W m^{-2}) vs the cumulative CO_2 emissions (Pg C) under the LH (blue) and HL (red) scenarios: (top left) net longwave radiative flux, (top right) upward latent heat flux, (middle left) net shortwave radiative flux, (middle right) upward sensible heat flux, (bottom left) net radiative flux, and (bottom right) adjusted net radiative flux. The markers are the annual mean and the solid lines are the 5-yr running-averaged fields.

the formation of North Atlantic Deep Water, which can transport the warmer surface water into the ocean bottom. Moreover, the sea ice feedbacks in the polar region may also be a reason for the deep ocean warming around 80°N.

Sea level height changed sterically (mainly due to thermal expansion) and eustatically (mainly owing to the changes of ice sheets and continental water storage) (Hansen et al. 2005). Since the total ice mass is related almost linearly to the cumulative CO_2 emissions and becomes a similar state under the LH and HL scenarios by the end of the simulation period (Fig. 7), herein the difference in sea level change is mainly attributed to the difference in ocean thermal expansion. In particular, by 2005, the differences of the full ocean temperature changes between the HL and LH scenarios yield an extra increase of about 4.7 cm in the mean steric sea level under the HL scenario, relative to the LH scenario. This indicates that reducing emissions earlier rather than later (i.e., under LH rather than HL), with the same quota and the same time period for the cumulative total CO_2 emissions, leads to a larger mitigation of ocean warming and sea level rise. Moreover, since there is a much larger carbon uptake by the ocean carbon pools under the HL scenario in the end of the simulated period, as discussed above, it can deduce that the ocean acidification will be more serious under this scenario.

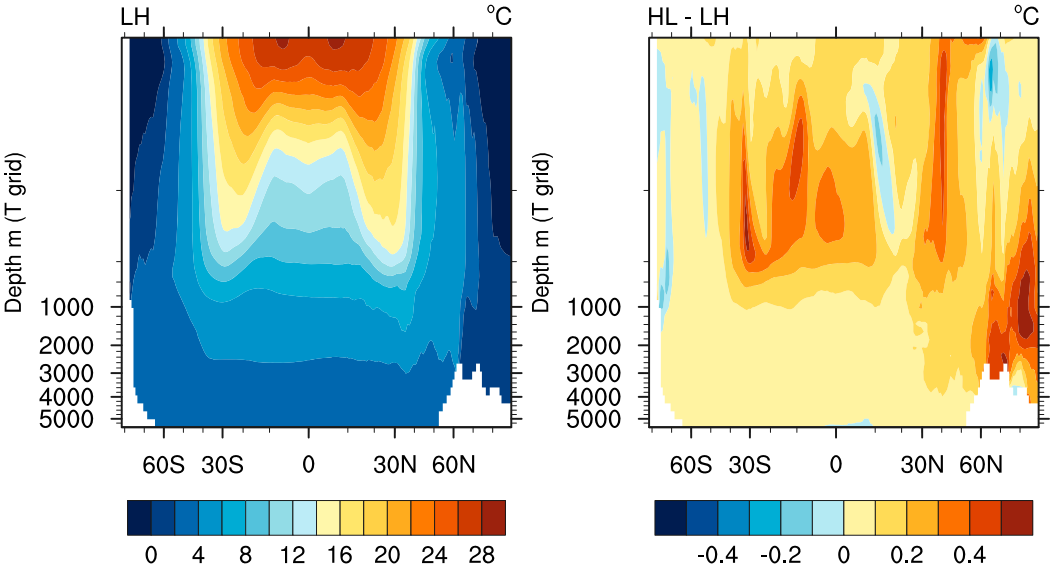

FIG. 6. The vertical structure of ocean potential temperature averaged over 1976–2005 (°C), simulated by (left) LH and (right) HL minus LH.

4. Discussion and conclusions

The transient climate response to cumulative CO_2 emissions is a useful policy framework as it establishes a simple relationship between the cause and the magnitude of warming. However, the responses of other facets of the climate system to cumulative CO_2 emissions and climate system responses to declining emissions scenarios are currently not well known. In this study, the fully coupled Earth system model, BNU-ESM, which incorporates the global carbon cycle, was used to investigate the climate system responses to a common emission budget of the historical industrial CO_2. Two numerical experiments were performed from 1850 to 2005 based on two different CO_2 emission scenarios: lower emissions earlier and higher emissions later (LH) and higher emissions earlier and lower emissions later (HL). Simulations with BNU-ESM demonstrate the following:

1) The carbon cycle feedbacks are carbon-emission scenario dependent. As to a given CO_2 emission budget and a given time period, the amount of land and ocean carbon sequestration will be larger under the HL scenario.
2) The responses of the processes within the atmosphere, land, and cryosphere are approximately linearly related to the cumulative CO_2 emissions under both the LH and HL scenarios. It is mainly attributed to the negative feedback between CO_2 radiative forcing and heat uptake by the land and ocean.
3) The processes with low climate sensitivities and large initial inertias, such as ocean warming and sea level rise, show a nonlinear relationship with the cumulative CO_2 emissions and are emission scenario dependent.

Herein, only the realized changes in climate system during the emission period are emphasized. The current definition of the final states is the end of the emissions period and neglects potentially important unrealized changes in some of the analyzed variables. Therefore, these results are relevant for centennial climate change when total cumulative CO_2 emissions reach the same total but not for long-term climate after emissions cease (Frölicher and Paynter 2015). In addition, the internal

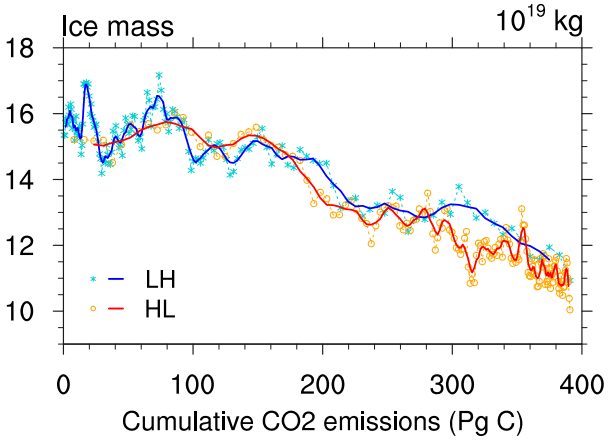

FIG. 7. Responses of ice mass (10^9 kg) vs the cumulative industrial CO_2 emissions (Pg C) under the LH (blue) and HL (red) scenarios. The markers are the annual mean and the solid lines are the 5-yr running-averaged fields.

variability is identified as one important source of the model uncertainty and could have a significant effect on the simulated results (Gillett et al. 2013). Because of the model internal variability and the nonlinearity of the climate system, the simulated changes of these climatic factors in the atmosphere, land, and cryosphere per unit CO_2 emission are not exactly constant in each scenario. The needed model time for achieving the same amount of cumulative CO_2 emissions is different under these two scenarios except at the end of the simulation, presumably resulting in slight differences in the corresponding changes of these variables for the same emission budget between the LH and HL scenarios.

The numerical results presented in this study show that the approximately linear relationship between the global warming quantified by the surface air temperature and cumulative CO_2 emissions can be extended to the Earth system model and to declining emissions scenarios. However, with a common emission target over a common time period, the ways of achieving the final climate state are different in the different CO_2 emission pathways, when faced with different climate risks. If the implementation of CO_2 emission reduction policies is delayed, like the HL scenario, Earth may experience earlier warming of the climate and may be at a greater risk, such as more severe ocean thermal expansion and ocean acidification. The full analyses of climate system response to different emission pathways leading to a common emission target can provide scientific directions for the reasonable allocation of the limited emission space and for the formation of emission reduction policies in the future.

Acknowledgments. This work was funded by the National Natural Science Foundation of China (41330527), the Key Laboratory of Earth Surface Processes and Resource Ecology (2013-ZY-02), and the National Natural Science Foundation of China (41505068).

REFERENCES

Allen, M. R., D. J. Frame, C. Huntingford, C. D. Jones, J. A. Lowe, M. Meinshausen, and N. Meinshausen, 2009: Warming caused by cumulative carbon emissions towards the trillionth tonne. *Nature*, **458**, 1163–1166, doi:10.1038/nature08019.

Andres, R. J., J. S. Gregg, L. Losey, G. Marland, and T. A. Boden, 2011: Monthly, global emissions of carbon dioxide from fossil fuel consumption. *Tellus*, **63B**, 309–327, doi:10.1111/j.1600-0889.2011.00530.x.

Archer, D., and Coauthors, 2009: Atmospheric lifetime of fossil fuel carbon dioxide. *Annu. Rev. Earth Planet. Sci.*, **37**, 117–134, doi:10.1146/annurev.earth.031208.100206.

Arora, V. K., and Coauthors, 2013: Carbon–concentration and carbon–climate feedbacks in CMIP5 Earth system models. *J. Climate*, **26**, 5289–5314, doi:10.1175/JCLI-D-12-00494.1.

Caldeira, K., and J. F. Kasting, 1993: Insensitivity of global warming potentials to carbon dioxide emission scenarios. *Nature*, **366**, 251–253, doi:10.1038/366251a0.

Cherubini, F., T. Gasser, R. M. Bright, P. Ciais, and A. H. Strømman, 2014: Linearity between temperature peak and bioenergy CO_2 emission rates. *Nat. Climate Change*, **4**, 983–987, doi:10.1038/nclimate2399.

Dong, W. J., F. M. Ren, J. B. Huang, and Y. Guo, 2013: *The Atlas of Climate Change: Based on SEAP-CMIP5*. Springer, 175 pp.

Dufresne, J.-L., and S. Bony, 2008: An assessment of the primary sources of spread of global warming estimates from coupled atmosphere–ocean models. *J. Climate*, **21**, 5135–5144, doi:10.1175/2008JCLI2239.1.

Eby, M., and Coauthors, 2013: Historical and idealized climate model experiments: An intercomparison of Earth system models of intermediate complexity. *Climate Past*, **9**, 1111–1140, doi:10.5194/cp-9-1111-2013.

Friedlingstein, P., and Coauthors, 2014: Persistent growth of CO_2 emissions and implications for reaching climate targets. *Nat. Geosci.*, **7**, 709–715, doi:10.1038/ngeo2248.

Frölicher, T. L., and D. J. Paynter, 2015: Extending the relationship between global warming and cumulative carbon emissions to multi-millennial timescales. *Environ. Res. Lett.*, **10**, 075002, doi:10.1088/1748-9326/10/7/075002.

——, M. Winton, and J. L. Sarmiento, 2014: Continued global warming after CO_2 emissions stoppage. *Nat. Climate Change*, **4**, 40–44, doi:10.1038/nclimate2060.

Gillett, N. P., V. K. Arora, K. Zickfeld, S. J. Marshall, and W. J. Merryfield, 2011: Ongoing climate change following a complete cessation of carbon dioxide emissions. *Nat. Geosci.*, **4**, 83–87, doi:10.1038/ngeo1047.

——, ——, D. Matthews, and M. R. Allen, 2013: Constraining the ratio of global warming to cumulative CO_2 emissions using CMIP5 simulations. *J. Climate*, **26**, 6844–6858, doi:10.1175/JCLI-D-12-00476.1.

Goodwin, P. G., R. Williams, and A. Ridgwel, 2015: Sensitivity of climate to cumulative carbon emissions due to compensation of ocean heat and carbon uptake. *Nat. Geosci.*, **8**, 29–34, doi:10.1038/ngeo2304.

Gregory, J. M., and P. M. Forster, 2008: Transient climate response estimated from radiative forcing and observed temperature change. *J. Geophys. Res.*, **113**, D23105, doi:10.1029/2008JD010405.

——, C. D. Jones, P. Cadule, and P. Friedlingstein, 2009: Quantifying carbon cycle feedbacks. *J. Climate*, **22**, 5232–5250, doi:10.1175/2009JCLI2949.1.

Hansen, J., and Coauthors, 2005: Earth's energy imbalance: Confirmation and implications. *Science*, **308**, 1431–1435, doi:10.1126/science.1110252.

——, and Coauthors, 2008: Target atmospheric CO_2: Where should humanity aim? *Open Atmos. Sci. J.*, **2**, 217–231, doi:10.2174/1874282300802010217.

Herrington, T., and K. Zickfeld, 2014: Path independence of climate and carbon cycle response over a broad range of cumulative carbon emissions. *Earth Syst. Dyn.*, **5**, 409–422, doi:10.5194/esd-5-409-2014.

IPCC, 2007: Summary for policymakers. *Climate Change 2007: The Physical Science Basis*, S. Solomon et al., Eds., Cambridge University Press, 1–18.

——, 2013: *Climate Change 2013: The Physical Science Basis*. Cambridge University Press, 1535 pp., doi:10.1017/CBO9781107415324.

Ji, D., and Coauthors, 2014: Description and basic evaluation of Beijing Normal University Earth System Model (BNU-ESM)

version 1. *Geosci. Model Dev.*, **7**, 2039–2064, doi:10.5194/gmd-7-2039-2014.

Joos, F., and Coauthors, 2013: Carbon dioxide and climate impulse response functions for the computation of greenhouse gas metrics: A multi-model analysis. *Atmos. Chem. Phys.*, **13**, 2793–2825, doi:10.5194/acp-13-2793-2013.

Knutti, R., and J. Rogelj, 2015: The legacy of our CO_2 emissions: A clash of scientific facts, politics and ethics. *Climatic Change*, **133**, 361–373, doi:10.1007/s10584-015-1340-3.

Krasting, J. P., J. P. Dunne, E. Shevliakova, and R. J. Stouffer, 2014: Trajectory sensitivity of the transient climate response to cumulative carbon emissions. *Geophys. Res. Lett.*, **41**, 2520–2527, doi:10.1002/2013GL059141.

Le Quéré, C., M. R. Raupach, J. G. Canadell, and G. Marland, 2009: Trends in the sources and sinks of carbon dioxide. *Nat. Geosci.*, **2**, 831–836, doi:10.1038/ngeo689.

MacDougall, A. H., and P. Friedlingstein, 2015: The origin and limits of the near proportionality between climate warming and cumulative CO_2 emissions. *J. Climate*, **28**, 4217–4230, doi:10.1175/JCLI-D-14-00036.1.

Matthews, H. D., and K. Caldeira, 2008: Stabilizing climate requires near-zero emissions. *Geophys. Res. Lett.*, **35**, L04705, doi:10.1029/2007GL032388.

——, N. P. Gillett, P. A. Stott, and K. Zickfeld, 2009: The proportionality of global warming to cumulative carbon emissions. *Nature*, **459**, 829–832, doi:10.1038/nature08047.

——, S. Solomon, and R. Pierrehumbert, 2012: Cumulative carbon as a policy framework for achieving climate stabilization. *Philos. Trans. Roy. Soc. London*, **370A**, 4365–4379, doi:10.1098/rsta.2012.0064.

Meinshausen, M., N. Meinshausen, W. Hare, S. C. B. Raper, K. Frieler, R. Knutti, D. J. Frame, and M. R. Allen, 2009: Greenhouse-gas emission targets for limiting global warming to 2°C. *Nature*, **458**, 1158–1162, doi:10.1038/nature08017.

Nohara, D., Y. Yoshida, K. Misumi, and M. Ohba, 2013: Dependency of climate change and carbon cycle on CO_2 emission pathways. *Environ. Res. Lett.*, **8**, 014047, doi:10.1088/1748-9326/8/1/014047.

Peng, J., W. Dong, W. Yuan, J. Chou, Y. Zhang, and J. Li, 2013: Effects of increased CO_2 on land water balance from 1850 to 1989. *Theor. Appl. Climatol.*, **111**, 483–495, doi:10.1007/s00704-012-0673-3.

Plattner, G.-K., and Coauthors, 2008: Long-term climate commitments projected with climate–carbon cycle models. *J. Climate*, **21**, 2721–2751, doi:10.1175/2007JCLI1905.1.

Ramanathan, V., and Y. Xu, 2010: The Copenhagen Accord for limiting global warming: Criteria, constraints, and available avenues. *Proc. Natl. Acad. Sci. USA*, **107**, 8055–8062, doi:10.1073/pnas.1002293107.

Raupach, M. R., 2013: The exponential eigenmodes of the carbon-climate system, and their implications for ratios of responses to forcings. *Earth Syst. Dyn.*, **4**, 31–49, doi:10.5194/esd-4-31-2013.

——, and Coauthors, 2014: Sharing a quota on cumulative carbon emissions. *Nat. Climate Change*, **4**, 873–879, doi:10.1038/nclimate2384.

Rogelj, J., D. L. McCollum, B. C. O'Neill, and K. Riahi, 2013: 2020 emissions levels required to limit warming to below 2°C. *Nat. Climate Change*, **3**, 405–412, doi:10.1038/nclimate1758.

Solomon, S., G.-K. Plattner, R. Knutti, and P. Friedlingstein, 2009: Irreversible climate change due to carbon dioxide emissions. *Proc. Natl. Acad. Sci. USA*, **106**, 1704–1709, doi:10.1073/pnas.0812721106.

——, J. S. Daniel, T. J. Sanford, D. M. Murphy, G.-K. Plattner, R. Knutti, and P. Friedlingstein, 2010: Persistence of climate changes due to a range of greenhouse gases. *Proc. Natl. Acad. Sci. USA*, **107**, 18 354–18 359, doi:10.1073/pnas.1006282107.

Wei, T., and Coauthors, 2012: Developed and developing world responsibilities for historical climate change and CO_2 mitigation. *Proc. Natl. Acad. Sci. USA*, **109**, 12 911–12 915, doi:10.1073/pnas.1203282109.

——, W. Dong, W. Yuan, X. Yan, and Y. Guo, 2014: Influence of the carbon cycle on the attribution of responsibility for climate change. *Chin. Sci. Bull.*, **59**, 2356–2362, doi:10.1007/s11434-014-0196-7.

Zickfeld, K., M. Eby, H. D. Matthews, and A. J. Weaver, 2009: Setting cumulative emissions targets to reduce the risk of dangerous climate change. *Proc. Natl. Acad. Sci. USA*, **106**, 16 129–16 134, doi:10.1073/pnas.0805800106.

——, and Coauthors, 2013: Long-term climate change commitment and reversibility: An EMIC intercomparison. *J. Climate*, **26**, 5782–5809, doi:10.1175/JCLI-D-12-00584.1.